PROTEIN STRUCTURE REPORT

Crystal structures of the extracellular domains of the CrRLK1L receptor-like kinases ANXUR1 and ANXUR2

Shuo Du, Li-Jia Qu, and Junyu Xiao*

The State Key Laboratory of Protein and Plant Gene Research, School of Life Sciences, Peking-Tsinghua Center for Life Sciences, Peking University, Beijing 100871, China

Received 19 November 2017; Accepted 30 January 2018
DOI: 10.1002/pro.3381
Published online 1 February 2018 proteinscience.org

Abstract: *Catharanthus roseus* Receptor-Like Kinase 1-like (CrRLK1L) proteins contain two tandem malectin-like modules in their extracellular domains (ECDs) and function in diverse signaling pathways in plants. Malectin is a carbohydrate-binding protein in animals and recognizes a number of diglucosides; however, it remains unclear how the two malectin-like domains in the CrRLK1L proteins sense the ligand molecule. In this study, we reveal the crystal structures of the ECDs of ANXUR1 and ANXUR2, two CrRLK1L members in *Arabidopsis thaliana* that have critical functions in controlling pollen tube rupture during the fertilization process. We show that the two malectin-like domains in these proteins pack together to form a rigid architecture. Unlike animal malectin, these malectin-like domains lack residues involved in binding to the diglucosides, suggesting that they have a distinct ligand-binding mechanism. A cleft is observed between the two malectin-like domains, which might function as a potential ligand-binding pocket.

Keywords: CrRLK1L; ANXUR1; ANXUR2; FERONIA; plant fertilization

Introduction

Receptor-like kinases (RLKs) play essential roles in a myriad of physiological processes in plants.[1–3] The general architecture of these proteins includes an N-terminal extracellular domain (ECD), a transmembrane region, and a C-terminal intracellular kinase domain. The ECDs perceive signaling cues, sometimes in the form of peptides and/or coreceptor proteins, and elicit cellular responses through the kinase domains. The *Catharanthus roseus* Receptor-Like Kinase 1-like (CrRLK1L) family of RLKs include 17 members in *Arabidopsis* and are characterized by the presence of two modules in their ECDs that bear sequence similarity to malectin, a glycan-binding protein in animals.[4–6] The charter member of this family is FERONIA (FER, At3g51550), a protein with multiple functions in fertilization, root growth, and immunity.[7–9] Due to the presence of the malectin-like domains, it was originally hypothesized that the CrRLK1L family proteins sense the glycan components in cell wall.[4,10] However, emerging evidence suggest that several small cysteine-rich peptides that belong to the rapid alkalization factor (RALF) family are ligands of FER, including RALF1 and RALF23.[11,12] Bacterially

Grant sponsor: National Key Research and Development Program of China; Grant numbers: 2017YFA0505200, 2016YFC0906000; Grant sponsor: National Natural Science Foundation of China; Grant number: 31570735.

*Correspondence to: Junyu Xiao, The State Key Laboratory of Protein and Plant Gene Research, School of Life Sciences, Peking-Tsinghua Center for Life Sciences, Peking University, Beijing 100871, China. E-mail: junyuxiao@pku.edu.cn

produced RALF1 and chemically synthesized RALF23 can initiate FER signaling in root development and immune response, suggesting that FER can recognize these proteins without glycosylation.

ANXUR1 (ANX1, At3g04690) and ANXUR2 (ANX2, At5g28680) are two other CrRLK1L member proteins and are the closest FER homologs among the 17 *Arabidopsis* CrRLK1Ls. ANX1 and ANX2 are highly similar to each other, sharing an overall 86% amino acid identity. Both are specifically localized at the tips of pollen tubes, where they have redundant functions in controlling pollen tube rupture and sperm cell release.[13,14] The ECD and kinase domain of ANX1 are 44% and 63% identical to those of FER, respectively.[15] Genetic experiments demonstrated that the kinase domains of the FER and ANX1 are interchangeable, whereas the ECDs are not, suggesting that they function through similar intracellular signaling pathways, but respond to different ligand molecules.[15] Recently, two other RALFs, RALF4 and RALF19, have been shown to be the ligands of ANX1 and ANX2,[16] suggesting that there is an intricate interplay between the RALFs and FER/ANX1/ANX2 during fertilization, and also raising the possibility that other CrRLK1L receptors may also recognize the RALF family peptides. Critical downstream components of ANX1/ANX2 signaling include the MARIS receptor-like cytoplasmic kinase and the NADPH oxidases RbohH and RbohJ, although the detailed signaling pathways remain to be delineated.[17,18]

Results and Discussion

Structures of ANX1 and ANX2 ECDs

The CrRLK1L family members are uniquely present in plants and do not have counterparts in animals. To date, they have not been characterized at the structural level. To gain insights into the function of this unique family of plant RLKs, we sought to determine the crystal structure of their ECDs. The ECDs of FER, ANX1, and ANX2 were expressed in insect cells and purified from conditioned media. All three proteins can be purified to homogeneity, however, only ANX1-ECD and ANX2-ECD were successfully crystallized. FER-ECD contains 10 predicted N-linked glycosylation sites, compared to five in ANX1 and four in ANX2 [Fig. 1(A)]. The large amount of glycans in FER-ECD likely hindered its crystallization, because of their inherent flexibility and heterogeneity. Although ANX1-ECD and ANX2-ECD contain two malectin-like domains [Mal-A and Mal-B, Fig. 1(A)], identities between them and malectin are very low (less than 20%), and we were not able to solve their structures using the molecular replacement method. We then prepared and crystallized selenomethionine (SeMet)-labeled ANX2-ECD and obtained experimental phases via the single wavelength anomalous diffraction method (Table I). The structure of ANX2-ECD was determined at 2.0 Å resolution, with an R-factor of 18.4% and an R_{free} of 20.8%, respectively. The structure of ANX1-ECD was subsequently determined at 1.8 Å via molecular replacement using ANX2-ECD as the search model [Table I, Fig. 1(B)]. The structures of ANX1-ECD and ANX2-ECD thoroughly resemble each other and can be superimposed with an rmsd (root mean square difference) of 0.6 Å over 383 aligned Cα atoms. We will focus on ANX1-ECD to illustrate the structural features of these two proteins below.

Although the two malectin-like domains in ANX1-ECD display only limited protein sequence similarity to malectin, their overall folds are similar to malectin and can be superimposed on malectin with rms differences of 2.7 Å over 139 aligned Cα atoms for Mal-A, and 2.9 Å over 151 aligned Cα atoms for Mal-B, respectively. They also show remarkable structural similarity to each other and can be superimposed with a rmsd of 2.0 Å over 149 aligned Cα atoms, despite the fact that they are only 19% identical in amino acid sequences. The core of each features a central jelly roll fold formed by two four-stranded β-sheets, which comprise strands β1 plus β6-β12 in Mal-A, and β15 plus β18-β24 in Mal-B [Fig. 1(B)]. The two domains are placed almost perpendicular to each other, with the C-terminal region of strand β10 in Mal-A packing against the N-terminal region of strand β15 in Mal-B. A β hairpin (β13-β14) links the two malectin-like domains and forms extensive interactions with Mal-B. The C-terminal tail of Mal-B folds back and intimately interacts with Mal-A. As a result of these interactions, the orientation of the two domains is fixed with respect to each other, and the overall ECD assembly appears to be rigid in nature.

Potential ligand-binding site

The physiological function of malectin in animal cells remains poorly understood; nevertheless, its carbohydrate-binding property has been rigorously characterized by Muhle-Goll and coworkers.[19,20] Malectin can bind to diglucosides in a variety of linkages using a surface pocket formed by several aromatic and acidic residues [Fig. 2(A)]. A structure-based sequence alignment suggests that the diglucoside-binding residues in malectin are not present in any of the malectin-like domains in ANX1, ANX2, and FER [Fig. 2(B)]. The surface areas of Mal-A and Mal-B in ANX1 that correspond to the diglucoside-binding pocket in malectin have different shapes; and when the two malectin-like domains in ANX1 are superimposed onto malectin, clashes will occur between ANX1 residues and the diglucoside [Fig. 2(C,D)]. The same is true for the Mal-A and Mal-B domains of ANX2, as well as the Mal-A of FER, when the structure of ANX2-ECD and a structure model of FER-ECD (generated by homology modeling based on the structure of ANX1-ECD) are examined. The Mal-B domain of FER contains a predicted

This figure also includes an iMolecules 3D interactive version that can be accessed via the link at the bottom of this figure's caption.

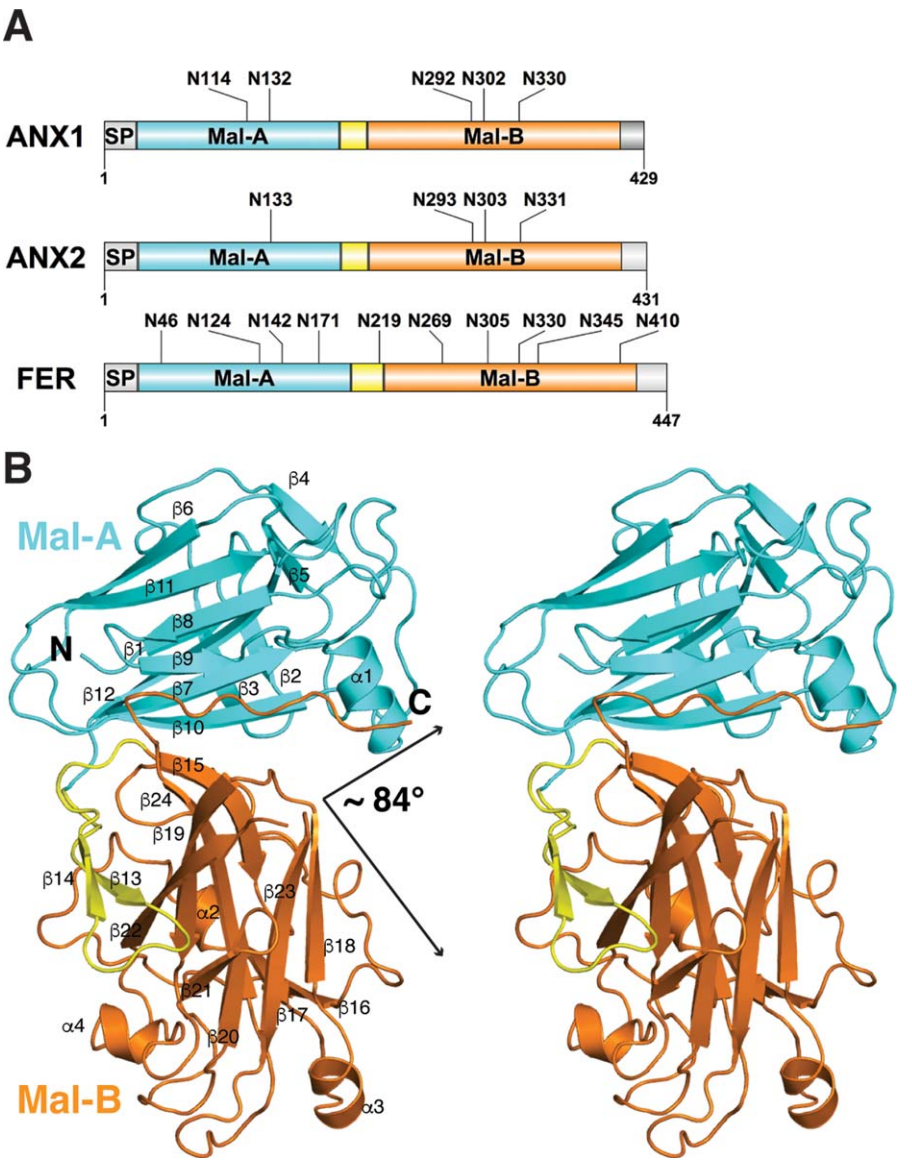

Figure 1. Crystal structure of the ANX1-ECD. (A) Schematic drawing of the ECDs of ANX1, ANX2, and FER. Mal-A domains are colored in cyan, Mal-B domains are colored in orange, and the linkers between them are colored in yellow. The predicted N-linked glycosylation sites are indicated. SP: signal peptide. (B) A stereo view of the Crystal structure of ANX1-ECD shown in the same color scheme as in (A). The N- and C-termini of the molecule, as well as the secondary structures are marked. An interactive view is available in the electronic version of the article.

glycosylation site (Asn330), and the glycan attached to this residue would impede the interaction with the diglucoside. Taken together, these analyses suggest that ANX1, ANX2, as well as FER would unlikely bind to diglucosides like malectin. Apparently, the malectin-like domains in these proteins have diverged greatly from animal malectin and perform different functions.

While it remains to be determined whether the "diglucoside-binding" pockets in the two malectin-like domains of ANX1, ANX2, and FER can bind to other molecules, a large cleft is present between Mal-A and Mal-B in ANX1 [Fig. 2(E)]. More than 50 residues contribute to the formation of this cleft, which has an estimated molecular surface of 1185 $Å^2$ and volume of 2019 $Å^3$, respectively, as calculated by the CASTp (Computed Atlas of Surface Topography of proteins) program.[23] Prominent residues guarding the entrance to this cleft include a group of hydrophobic amino acids: Leu72, Ala141, Leu142, Tyr146, Phe214, Pro224, Tyr237, Tyr242, Pro406, and Pro408 [Fig. 2(E)]. Exposure of large number of hydrophobic residues is energetically unfavorable for soluble proteins, and such surface areas usually indicate binding sites for other molecules. Besides these hydrophobic residues, many hydrophilic residues also reside in this region, such as Gln42,

Table I. *Data Collection and Refinement Statistics*

Data collection	ANX1	ANX2	SeMet ANX2
Space group	*P*1	*I*4	*I*4
Cell dimensions	$a = 54.68$ Å, $b = 68.74$ Å, $c = 70.33$ Å, $\alpha = 88.95°$, $\beta = 75.00°$, $\gamma = 72.18°$	$a = 103.19$ Å, $b = 103.19$ Å, $c = 121.74$ Å, $\alpha = 90°$, $\beta = 90°$, $\gamma = 90°$	$a = 102.20$ Å, $b = 102.20$ Å, $c = 121.79$ Å, $\alpha = 90°$, $\beta = 90°$, $\gamma = 90°$
Wavelength (Å)	0.9785	0.9779	0.9790
Resolution (Å)	1.8	2.0	2.5
R_{merge}	0.088 (0.208)	0.092 (0.606)	0.133 (0.956)
$I/\sigma I$	17.3 (6.8)	34.7 (2.8)	18.0 (2.1)
Completeness (%)	96.5 (95.4)	100 (99.5)	99.9 (100.0)
Multiplicity	3.5 (3.5)	13.3 (10.9)	6.2 (6.2)
Wilson B-factor (Å^2)	20.41	42.71	41.39
Refinement			
Unique reflections	83947	42701	
R_{work}/R_{free}	0.181/0.207	0.184/0.208	
Number of atoms			
Protein	5998	3015	
Ligand	126	120	
Solvent	829	105	
Protein residues	763	396	
B-factors (Å^2)			
Protein	28.07	56.55	
Ligand	48.03	97.29	
Solvent	41.08	54.89	
R.m.s deviations			
Bond lengths (Å)	0.003	0.009	
Bond angles (°)	0.83	1.09	
Ramachandran			
Favored (%)	96.83	96.10	
Allowed (%)	3.17	3.38	
Outliers (%)	0.00	0.52	

Each dataset was collected from a single crystal. Values in parentheses are for highest-resolution shell.

Asp43, Lys45, Gln144, Thr233, Thr235, Gln298, Lys301, Glu368, and Glu409 [Fig. 2(E)]. These hydrophilic residues would ensure the binding specificity by providing ionic and hydrogen bond interactions. For these reasons, we envision that the central cleft between Mal-A and Mal-B might function as a binding site for potential ligands. FER-ECD is expected to have a similar cleft. Interestingly, however, many "mouth" residues mentioned above are occupied by different amino acids in FER [Fig. 2(F)]. This would lead to distinct binding specificities for ANX1/ANX2 and FER towards their respective ligand molecules.

In summary, we have determined the crystal structures of the extracellular domains of ANX1 and ANX2, thereby providing the first structural information for the CrRLK1L family of RLKs in plants. Our results show that the two malectin-like domains in these proteins are arranged in a perpendicular manner and form a rigid assembly. Importantly, detailed structural analyses suggest that the malectin-like domains in ANX1, ANX2, and FER would unlikely bind to diglucosides like animal malectin. In contrast, a central cleft between the two malectin-like domains might serve as an ideal ligand-binding site. These results provide a starting point to further pinpoint the physiological function of these important receptor molecules in plants, and also serve as templates for future analyses of the receptor-ligand complexes.

Materials and Methods

Protein expression and purification

ANX1-ECD (residues 27–427) and ANX2-ECD (residues 28–431) with C-terminal 6 × His tags were cloned into a modified pFastBac-Dual vector (Invitrogen) that encodes an N-terminal melittin signal peptide. Recombinant baculoviruses were generated and amplified using the sf21 insect cells (maintained in the SIM SF medium, Sino Biological) following standard procedures (Bac-to-Bac, Invitrogen). One liter of High Five (Hi5) insect cells (1.5×10^6 cells mL^{-1}, cultured in the SIM HF medium, Sino Biological) was infected with 5 mL recombinant baculoviruses. The conditioned medium was harvested after 48 h, concentrated using a Hydrosart Ultrafilter (Sartorius), and exchanged into the binding buffer containing 25 m*M* Tris-HCl (pH = 8.0) and 150 m*M* NaCl. The fusion proteins were then purified using the Ni-NTA resin (GE healthcare), ion-exchange column (RESOURCEQ, GE Healthcare), and size-exclusion column (Superdex 200 increase, GE Healthcare). The final protein buffer contains 25 m*M* Tris (pH = 8.0) and 150 m*M* NaCl.

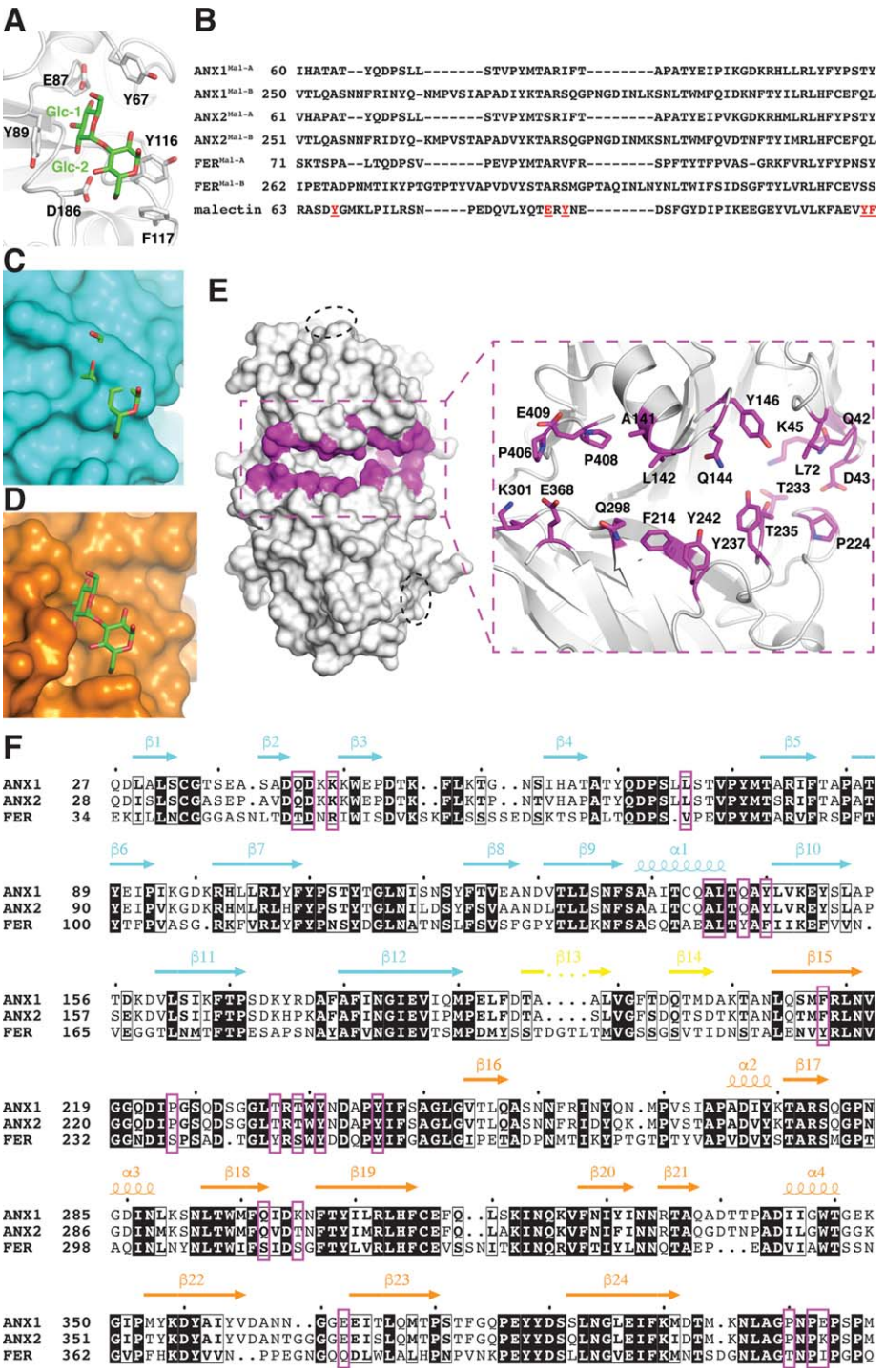

Figure 2. Potential ligand binding-site in ANX1-ECD. (A) A surface pocket in malectin binds to the diglucosides. The structure of malectin in complex with the diglucoside nigerose (Glcα1–3Glc, PDB ID: 2K46) is shown as ribbon diagrams. The carbon atoms in malectin and nigerose are shown in white and green, respectively; and the oxygen atoms are shown in red. Residues involved in binding to the nigerose are highlighted. (B) The diglucoside-binding residues in malectin are not present in any of the malectin-like domains in ANX1, ANX2, and FER. The structure-based sequence alignment is generated using PROMALS3D.[21] Diglucoside-binding residues in malectin are highlighted in red and underlined. (C, D) Residues in the Mal-A (cyan) and Mal-B (orange) domains of ANX1-ECD would collide with the diglucoside, when Mal-A and Mal-B are superimposed onto the malectin-nigerose complex shown in (A). (E) A potential ligand-binding cleft in ANX1-ECD. Prominent residues involved in forming the central cleft between Mal-A and Mal-B are highlighted in magenta and labeled. The regions in Mal-A and Mal-B that correspond to the diglucoside-binding pocket in malectin are indicated with dashed ovals. (F) Sequence alignment of the ECDs of ANX1, ANX2, and FER. Secondary structure elements of ANX1-ECD are shown above the sequence blocks and colored like in Figure 1(B). Residues involved in forming the central cleft between Mal-A and Mal-B are highlighted with magenta boxes. The figure was prepared using ESPript.[22]

To generate selenomethionine (SeMet) substituted ANX2-ECD, Hi5 cells were adapted to a methionine-free medium (ESF 921 methionine-deficient, Expression Systems) and infected with baculovirus.[24] The culture was supplemented twice with 100 mg/L SeMet (ACROS) at 12 and 36 h postinfection. The conditioned media were then harvested and the SeMet ANX2-ECD purified as described above.

Crystallization

For crystallization, ANX1-ECD and ANX2-ECD were concentrated to 12 and 13 mg/mL, respectively. All crystals were grown at 20°C using the sitting-drop vapor diffusion method. The crystallization solution of ANX1-ECD contains 0.2*M* ammonium acetate, 0.1*M* HEPES (pH = 7.5), and 25% (w/v) polyethylene glycol (PEG) 3350. For data collection, the ANX1-ECD crystals were transferred to a solution containing 0.2*M* ammonium acetate, 0.1*M* HEPES (pH = 7.5), 25% (w/v) PEG 3350, and 10% ethylene glycol, and frozen in liquid nitrogen. The crystallization solution of ANX2-ECD contains 0.2*M* Li_2SO_4, 0.1*M* sodium acetate (pH = 4.5), and 50% PEG 400. The ANX2-ECD crystals were flash-frozen in liquid nitrogen directly. The SeMet ANX2-ECD protein was concentrated to 6 mg/mL and used for crystallization. The SeMet ANX2-ECD crystals were grown in 0.2*M* Li_2SO_4, 0.1*M* sodium acetate (pH = 5.0), and 48% PEG400, and flash-frozen in liquid nitrogen directly.

Structure determination

The diffraction data were collected at the Shanghai Synchrotron Radiation Facility (beamline BL17U)[25] and the National Facility for Protein Science Shanghai (beamline BL19U). The data were indexed, integrated, and scaled using the HKL2000 program (HKL Research). The ANX2-ECD structure was determined by the single-wavelength dispersion method using data collected from a SeMet crystal. Heavy atom search, phase calculation and refinement, and density modification were carried out with Phenix.[26] Initial model building was performed using ARP/wARP.[27] The structural model was further built in Coot[28] and refined using Phenix. The ANX1-ECD structure was determined by molecular replacement using Phaser,[29] with the ANX2-ECD structure as the initial search model, and refined using Phenix.

Acknowledgments

We are grateful to the staff of the Shanghai Synchrotron Radiation Facility (beamline BL17U) and the National Facility for Protein Science Shanghai (beamline BL19U) for assistance with X-ray data collection.

Author Contributions

Li-Jia Qu and Junyu Xiao designed the project. Shuo Du performed all the experiments, including protein expression, purification, and crystallization. Junyu Xiao performed crystallography and structural analyses and wrote the manuscript.

Conflict of Interest

The authors declare no conflict of interest.

Data Availability

Atomic coordinates and structural factors have been deposited in the Protein Data Bank with accession codes 5Y96 and 5Y92 for ANX1-ECD and ANX2-ECD, respectively.

References

1. Shiu SH, Bleecker AB (2001) Plant receptor-like kinase gene family: diversity, function, and signaling. Sci STKE 2001:re22.
2. De Smet I, Voss U, Jurgens G, Beeckman T (2009) Receptor-like kinases shape the plant. Nat Cell Biol 11: 1166–1173.
3. Song W, Han Z, Wang J, Lin G, Chai J (2017) Structural insights into ligand recognition and activation of plant receptor kinases. Curr Opin Struct Biol 43:18–27.
4. Boisson-Dernier A, Kessler SA, Grossniklaus U (2011) The walls have ears: the role of plant CrRLK1Ls in sensing and transducing extracellular signals. J Exp Bot 62:1581–1591.
5. Lindner H, Muller LM, Boisson-Dernier A, Grossniklaus U (2012) CrRLK1L receptor-like kinases: not just another brick in the wall. Curr Opin Plant Biol 15:659–669.
6. Nissen KS, Willats WG, Malinovsky FG (2016) Understanding CrRLK1L function: cell walls and growth control. Trends Plant Sci 21:516–527.
7. Kessler SA, Grossniklaus U (2011) She's the boss: signaling in pollen tube reception. Curr Opin Plant Biol 14:622–627.
8. Qu LJ, Li L, Lan Z, Dresselhaus T (2015) Peptide signalling during the pollen tube journey and double fertilization. J Exp Bot 66:5139–5150.
9. Liao H, Tang R, Zhang X, Luan S, Yu F (2017) FERONIA receptor kinase at the crossroad of hormone signaling and stress responses. Plant Cell Physiol 58:1143–1150.
10. Cheung AY, Wu HM (2011) THESEUS 1, FERONIA and relatives: a family of cell wall-sensing receptor kinases? Curr Opin Plant Biol 14:632–641.
11. Haruta M, Sabat G, Stecker K, Minkoff BB, Sussman MR (2014) A peptide hormone and its receptor protein kinase regulate plant cell expansion. Science 343:408–411.
12. Stegmann M, Monaghan J, Smakowska-Luzan E, Rovenich H, Lehner A, Holton N, Belkhadir Y, Zipfel C (2017) The receptor kinase FER is a RALF-regulated scaffold controlling plant immune signaling. Science 355:287–289.
13. Miyazaki S, Murata T, Sakurai-Ozato N, Kubo M, Demura T, Fukuda H, Hasebe M (2009) ANXUR1 and 2, sister genes to FERONIA/SIRENE, are male factors for coordinated fertilization. Curr Biol 19:1327–1331.
14. Boisson-Dernier A, Roy S, Kritsas K, Grobei MA, Jaciubek M, Schroeder JI, Grossniklaus U (2009) Disruption of the pollen-expressed FERONIA homologs ANXUR1 and ANXUR2 triggers pollen tube discharge. Development 136:3279–3288.
15. Kessler SA, Lindner H, Jones DS, Grossniklaus U (2015) Functional analysis of related CrRLK1L

receptor-like kinases in pollen tube reception. EMBO Rep 16:107–115.
16. Ge Z, Bergonci T, Zhao Y, Zou Y, Du S, Liu MC, Luo X, Ruan H, Garcia-Valencia LE, Zhong S, Hou S, Huang Q, Lai L, Moura DS, Gu H, Dong J, Wu HM, Dresselhaus T, Xiao J, Cheung AY, Qu LJ (2017) Arabidopsis pollen tube integrity and sperm release are regulated by RALF-mediated signaling. Science 358:1596–1600.
17. Boisson-Dernier A, Lituiev DS, Nestorova A, Franck CM, Thirugnanarajah S, Grossniklaus U (2013) ANXUR receptor-like kinases coordinate cell wall integrity with growth at the pollen tube tip via NADPH oxidases. PLoS Biol 11:e1001719.
18. Boisson-Dernier A, Franck CM, Lituiev DS, Grossniklaus U (2015) Receptor-like cytoplasmic kinase MARIS functions downstream of CrRLK1L-dependent signaling during tip growth. Proc Natl Acad Sci U S A 112:12211–12216.
19. Schallus T, Jaeckh C, Feher K, Palma AS, Liu Y, Simpson JC, Mackeen M, Stier G, Gibson TJ, Feizi T, Pieler T, Muhle-Goll C (2008) Malectin: a novel carbohydrate-binding protein of the endoplasmic reticulum and a candidate player in the early steps of protein *N*-glycosylation. Mol Biol Cell 19:3404–3414.
20. Schallus T, Feher K, Sternberg U, Rybin V, Muhle-Goll C (2010) Analysis of the specific interactions between the lectin domain of malectin and diglucosides. Glycobiology 20:1010–1020.
21. Pei J, Kim BH, Grishin NV (2008) PROMALS3D: a tool for multiple protein sequence and structure alignments. Nucleic Acids Res 36:2295–2300.
22. Robert X, Gouet P (2014) Deciphering key features in protein structures with the new ENDscript server. Nucleic Acids Res 42:W320–W324.
23. Dundas J, Ouyang Z, Tseng J, Binkowski A, Turpaz Y, Liang J (2006) CASTp: computed atlas of surface topography of proteins with structural and topographical mapping of functionally annotated residues. Nucleic Acids Res 34:W116–W118.
24. Xiao J, Tagliabracci VS, Wen J, Kim SA, Dixon JE (2013) Crystal structure of the Golgi casein kinase. Proc Natl Acad Sci U S A 110:10574–10579.
25. Wang QS, Yu F, Huang S, Sun B, Zhang KH, Liu K, Wang ZJ, Xu CY, Wang SS, Yang LF, Pan QY, Li L, Zhou H, Cui Y, Xu Q, Earnest T, He JH (2015) The macromolecular crystallography beamline of SSRF. Nucl Sci Tech 26:12–17.
26. Adams PD, Afonine PV, Bunkoczi G, Chen VB, Davis IW, Echols N, Headd JJ, Hung LW, Kapral GJ, Grosse-Kunstleve RW, McCoy AJ, Moriarty NW, Oeffner R, Read RJ, Richardson DC, Richardson JS, Terwilliger TC, Zwart PH (2010) PHENIX: a comprehensive Python-based system for macromolecular structure solution. Acta Cryst 66:213–221.
27. Carolan CG, Lamzin VS (2014) Automated identification of crystallographic ligands using sparse-density representations. Acta Cryst D70:1844–1853.
28. Emsley P, Lohkamp B, Scott WG, Cowtan K (2010) Features and development of Coot. Acta Cryst 66:486–501.
29. McCoy AJ, Grosse-Kunstleve RW, Adams PD, Winn MD, Storoni LC, Read RJ (2007) Phaser crystallographic software. J Appl Cryst 40:658–674.